

Self-Association of Spectrin's Repeating Segments[†]Greg Ralston,^{*,‡} Timothy J. Cronin,[§] and Daniel Branton[§]*Department of Biochemistry, University of Sydney, Sydney, NSW 2006, Australia, and Department of Molecular and Cellular Biology, Harvard University, 16 Divinity Avenue, Cambridge, Massachusetts 02138**Received September 18, 1995; Revised Manuscript Received January 8, 1996[®]*

ABSTRACT: We have examined the self-association behavior in solution of one of the repeating conformational segments of *Drosophila* spectrin, D- α -14, as well as of the two-segment unit, D- α -14,15. In both polypeptides, sedimentation equilibrium and nondenaturing gel electrophoresis detect a reversible, moderate affinity ($K_2 \cong 10^4 \text{ M}^{-1}$) dimerization reaction. Equilibration between monomer and dimer is kinetically limited near 5 °C, but occurs at a measurable rate at temperatures ≥ 20 °C. The temperature dependence for equilibration is consistent with the requirement for extensive disruption of helix–helix packing as the reaction proceeds in either direction. Hydrodynamic studies by means of sedimentation velocity confirm that in solution the C helix in the monomer of D- α -14 is folded back to interact with the A and B helices, and that the form of the monomeric subunit observed in the crystal structure, in which the B and C helices are continuous, does not persist in the monomer in solution. Both the dimer of D- α -14 and the monomer of D- α -14,15 appear to be twice the length of the D- α -14 monomer, while the frictional ratio of the D- α -14,15 dimer is consistent with four end-to-end triple α -helical domains.

Proteins in the spectrin family contain a series of homologous, tandemly repeating conformational segments, each containing approximately 106 amino acids. The spectral properties of the protein and the sequence of each segment predict that a conformational unit consists of three α -helices connected by two β -turns (Speicher *et al.*, 1980; Speicher & Marchesi, 1984). Fragments of spectrin cDNA encoding single segments and pairs of segments can be expressed in *Escherichia coli*, and, depending on the phasing of the expressed polypeptides, these polypeptides do fold into stable conformations whose properties are similar to those of the repeating segments in the intact spectrin molecule (Winograd *et al.*, 1991).

The X-ray crystal structure of one of these repeating segments, the 14th segment from the α -chain of *Drosophila* spectrin (D- α -14), has been determined (Yan *et al.*, 1993). Surprisingly, D- α -14 crystallized as a dimer, in which the third helix (the C helix) of the first polypeptide interacted with the A and B helices of the second polypeptide in what were presumed to be precisely the same contacts as occur in the intact spectrin molecule. In the intact molecule, where segment dimers cannot exist, the C helix of each segment is presumed to fold back and pack against the A and B helices within the same segment, thus forming a three-helix bundle (Yan *et al.*, 1993).

The existence of spectrin dimers in the crystals was explained by Yan *et al.* (1993) by reference to unpublished observations indicating that the D- α -14 segment existed in solution as mixtures of monomers and homodimers whose

rate of interconversion was slow. We have now completed a detailed examination of the self-association behavior of D- α -14 in solution by means of sedimentation equilibrium. At temperatures above 20 °C, we detected a reversible dimerization reaction of moderate affinity. At low temperatures, the reaction was kinetically trapped. Sedimentation velocity studies were employed to resolve the folding mode within the monomers and to investigate the gross conformation of the various oligomers. We have also examined the behavior of a two-segment polypeptide, D- α -14,15, comprising the 14th and 15th conformational units in tandem. All of the results are consistent with the three-helix bundle assumed by Yan *et al.* (1993) for the intact molecule.

MATERIALS AND METHODS

Expression and Purification of Protein. The recombinant fragments of spectrin cDNA encoding either *Drosophila* spectrin segment 14 [D- α -14, originally called B14 by Winograd *et al.* (1991)] or *Drosophila* spectrin segments 14 and 15 (D- α -14,15, originally called B14–15) were expressed in *E. coli* as glutathione transferase–spectrin fusion proteins. The glutathione transferase–D- α fusion proteins were bound to glutathione–agarose beads (Sigma), and the D- α fragments were cleaved off the bead with thrombin (Winograd *et al.*, 1991). The fragments were further purified in a 4 °C room on a Mono Q column (Pharmacia FPLC system) from which they eluted as two distinct peaks. For the studies reported here, the two peaks were dealt with separately and called peak 1 and peak 2. Peak fractions were collected on ice and dialyzed at 4 °C for a 40 h period with three changes of buffer against 40 mM Tris-HCl, pH 7.5, with or without 100 mM NaCl.

Protein samples prepared at Harvard University were transported on dry ice to the analytical ultracentrifuge laboratory at the University of Sydney, either in 50% glycerol solution or as lyophilized powders, and were stored at –20 °C prior to use.

[†] This study was supported by the Australian Research Council, by the University of Sydney (to G.R.), and by National Institutes of Health Grant HL17411 (to D.B.).

* Correspondence should be addressed to this author at the Department of Biochemistry, University of Sydney, Sydney, NSW 2006, Australia. Telephone: 61 2 351 3906. Fax: 61 2 351 4726. E-mail: G.Ralston@biochem.usyd.edu.au.

[‡] University of Sydney.

[§] Harvard University.

[®] Abstract published in *Advance ACS Abstracts*, April 1, 1996.

Analytical Ultracentrifugation. Samples for sedimentation analysis were dialyzed for at least 24 h against the appropriate buffer with or without supporting electrolyte. Tris buffer was used in most cases, with no observable differences in the protein behavior between 5 mM and 40 mM Tris. Dithiothreitol, 0.1 mM, was added to all buffers to minimize oxidation of sulfhydryl groups, and the buffers were thoroughly purged of oxygen by sparging with N₂ gas for 15 min. Dialysis was performed in screw-cap Pyrex bottles with minimum headspace. The dialysate was used for preparing dilutions.

Sedimentation Equilibrium. Samples (120 μ L) of the dialyzed protein solution at three different dilutions (usually 0.2, 0.1, and 0.05 g/L) were placed in the sample channels of an ultracentrifuge cell fitted with a Yphantis 6-channel centerpiece. For use with the Model E ultracentrifuge, sample loadings up to 1.0 g/L were employed. Aliquots of the dialysate (120 μ L) were placed in the reference channels. The samples were centrifuged at various angular velocities in a Beckman XL-A analytical ultracentrifuge, at temperatures between 4 °C and 37 °C, or in a Beckman Model E analytical ultracentrifuge, at temperatures between 4 °C and 30 °C. In experiments at different temperatures, sedimentation equilibrium was first attained at the lowest temperature, after which the temperature was raised, and sedimentation was continued.

In experiments with the XL-A instrument, scans were taken at wavelengths between 225 and 280 nm, depending on the sample concentrations, and a base-line scan was taken at 360 nm to correct, where necessary, for optical imperfections or partial masking of light pulses. Scans were taken at 4 h intervals, and sedimentation equilibrium was deemed to have been reached when the difference between consecutive scans was zero, within the precision of the measurements, indicating no significant change in concentration distribution. The calculated time to equilibrium (Teller, 1973) was between 14 and 32 h, depending on the protein species and the rotor speed. In all cases, the actual time of centrifugation was greater than the calculated time.

For experiments in the Model E instrument, Rayleigh interference patterns were photographed at 4000 rpm during acceleration, and periodically after 24 h at the set speed, the length of the interval depending on the temperature used. The pattern at zero time was used to correct for cell and window distortion (Teller, 1973).

Data Treatment. The equilibrium distributions were analyzed in several ways: by fitting of the absorbance versus radial distance distribution, using the program NONLIN (Johnson *et al.*, 1981); through calculation of the apparent weight-average molecular weight, $M_{w,app}$; or by means of the Omega function (Milthorpe *et al.*, 1975; Morris & Ralston, 1985; Ralston & Morris, 1992).¹ The Omega function (Milthorpe *et al.*, 1975) for a nonideal, self-associating solute is a continuous function of the total concentration of associating solute at any point in the centrifuge cell, independent of rotor speed, radial position, or initial loading concentration, and may be expressed:

$$\Omega(r) = a_1(r_F)c(r)/c(r_F)a_1(r)$$

where $a_1(r)$ is the thermodynamic activity of the monomer at radial distance r . If chemical and sedimentation equilibrium are attained, and all solute species take part in the reaction, the Omega function distributions from experiments with different loading concentrations and at different rotor speeds will overlap, and the continuous curve is a function of the parameters of the association reaction: the equilibrium constants and the second virial coefficient (Milthorpe *et al.*, 1975; Morris & Ralston, 1985). Since the Omega function does not require differentiation of the data (as is required with the calculation of the point-average weight-average molecular weight), the Omega distribution conveys information at a greater signal to noise ratio than the corresponding distribution of $M_{w,app}$.

For the Omega calculations, a reference concentration was chosen common to all three channels in a given experiment. This allows testing for coincidence of the Omega distributions as a check on attainment of equilibrium and the absence of contaminants. The Omega and $M_{w,app}$ data were fitted with reaction models² (Teller, 1973; Ralston & Morris, 1992) to estimate the equilibrium constants for the association reactions and the degree of nonideality. In those cases where chemical equilibrium was not attained and nonideality was not pronounced, the program MULTMX3B³ was used to estimate the proportions of different oligomeric species in the samples.

Sedimentation Velocity. Sedimentation velocity experiments were carried out at 58 000–60 000 rpm in the XL-A instrument at the stated temperature and with the use of standard aluminum double-sector cells. The data were analyzed by means of the program SVEDBERG (Philo, 1994),⁴ which enables simultaneous fitting of up to nine scans with a model comprising up to three distinct sedimenting species. This program returns the sedimentation and diffusion coefficients, and the relative concentrations of each species, and allows for a base-line offset to account for nonsedimenting absorbance. In some experiments, scans were collected every 5 min, and the distributions of apparent sedimentation coefficients, $g(s^*)$, were computed by the method of Stafford (1992, 1994).

The sedimentation and diffusion coefficients of the various oligomers were modeled with arrays of contiguous spheres with the use of the program HYDRO (García de la Torre *et al.*, 1994).

Polyacrylamide Gel Electrophoresis. The oligomeric state of the dialyzed protein samples from peaks 1 and 2 was examined using a nondenaturing, nonreducing tricine gel system [recipe of Schagger and Jagow (1987) but without SDS] containing 4% total acrylamide, 3% bis(acrylamide) cross-linker stacking gel and a 10% acrylamide, 3% bis(acrylamide) resolving gel with "cathode" buffer in both upper and lower reservoirs. A total of 2 μ g of each sample was loaded and electrophoresed at an average of 17 mA, at

¹ $\Omega(r) = c(r) \exp[\phi_1(M_1(r_F^2 - r^2))/c(r_F)]/c(r_F)$, where $c(r)$ is the total solute concentration at radial distance r , M_1 the molar mass of the monomer, and $\phi_1 = (1 - \nu\rho)\omega^2/2RT$, with ν the partial specific volume, ρ the solvent density, ω the angular velocity, and r_F an arbitrary reference position in the cell.

² A group of programs named SEDPROG, for analysis of Omega and $M_{w,app}$ distributions, is available from the RASMB ftp server, bbri.harvard.edu.

³ The program MULTMX3B, for analysis of mixtures not in equilibrium, was written by Allen Minton, NIH, and is available on the RASMB ftp server, bbri.harvard.edu.

⁴ The program SVEDBERG was written by John Philo, Amgen Inc., and is available on the RASMB ftp server, bbri.harvard.edu.

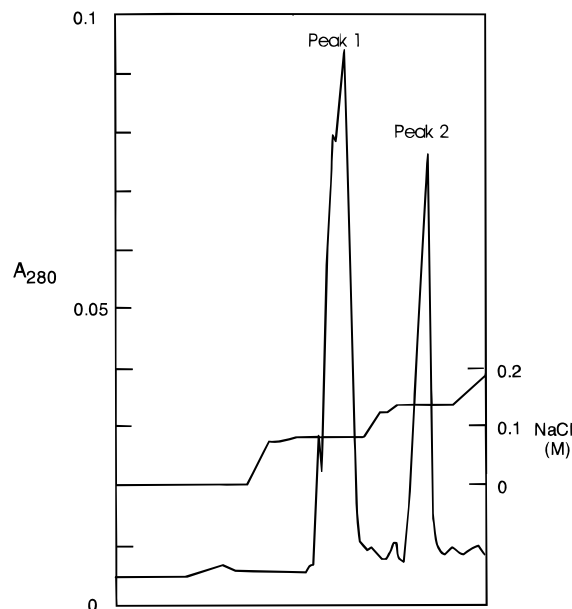


FIGURE 1: Elution profile of the D- α -14 spectrin segment from a Mono Q 5/5 column. Six milligrams of the protein was loaded at a concentration of 4.4 mg/mL in 40 mM Tris-HCl, pH 7.5, and was eluted with a programmed gradient of NaCl in 40 mM Tris-HCl, pH 7.5.

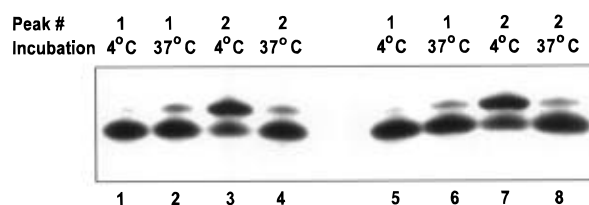


FIGURE 2: Gel electrophoresis of D- α -14 protein at 5 °C. The proteins at 0.25 mg/mL in 40 mM Tris-HCl, pH 7.5, either with or without 100 mM NaCl, from peak 1 or peak 2, either held at 4 °C or after 6 h incubation at 37 °C, as indicated, were electrophoresed on a Tris/Tricine gel. Lanes 1–4, without NaCl; lanes 5–8, with 100 mM NaCl.

constant current, for approximately 9 h. The temperatures of the buffer in the upper reservoir and the gel itself were maintained below 5 °C throughout the run by packing ice in a contiguous compartment.

RESULTS

Characterization of the Peak 1 and Peak 2 Material. Preparation of the D- α -14 unit routinely yielded two peaks on ion exchange chromatography from Mono Q (Figure 1). The first peak (peak 1) eluted at 80 mM NaCl and, when maintained at 4 °C, gave rise predominantly to a single band on nondenaturing gel electrophoresis (Figure 2, lanes 1, 5). The second peak (peak 2) eluted at 135 mM NaCl and, when maintained at 4 °C, gave rise to two bands: a major band of lesser mobility than the peak 1 material, and a minor band of mobility equal to that of peak 1 material (Figure 2, lanes 3, 7). In denaturing SDS-PAGE, both peaks give rise to a single peak with $M_r \approx 12\,500$ (Winograd *et al.*, 1991).

Sedimentation equilibrium in the presence of 50–100 mM NaCl showed that, when maintained below 20 °C, peak 1 material was mostly a monomer species of molecular mass ca. 12 kDa that contained only traces of higher molecular weight material, presumably dimer (Figure 3a). On the other hand, similar low-temperature storage and sedimentation

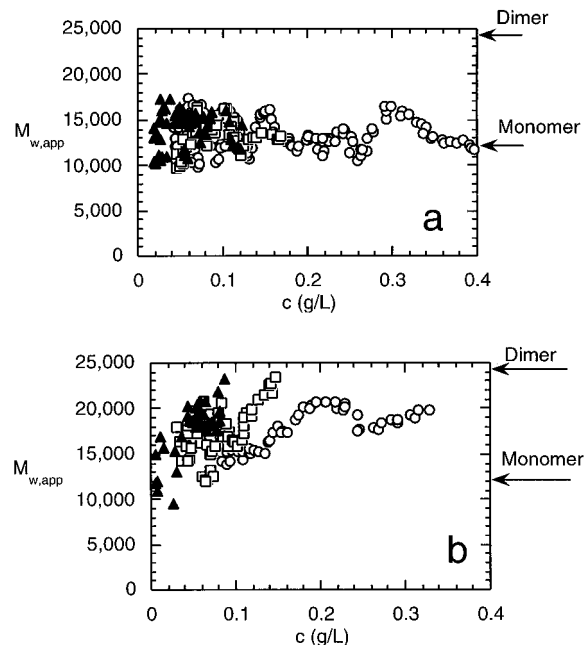


FIGURE 3: Sedimentation equilibrium at 5 °C of (a) peak 1 and (b) peak 2 material in 50 mM Tris-HCl, 0.1 M NaCl, pH 7.5. Initial loading concentrations: (\blacktriangle) 0.05 g/L; (\square) 0.1 g/L; (\circ) 0.2 g/L. (a) Peak 1 protein showed a weight-average molecular mass of approximately 12 kDa across the entire cell, and independent of the initial loading concentration. (b) Peak 2 material showed increasing $M_{w,app}$ from that of the monomer, 12 kDa, near the meniscus, rising toward 24 kDa near the cell bottom. Data from different loading concentrations did not overlap, indicating heterogeneity.

equilibrium measurements showed that peak 2 was heterogeneous. With increasing concentration through the centrifuge cell, the apparent weight-average molecular mass of the peak 2 material rose from that of the monomer (ca. 12 kDa) toward that of the dimer (ca. 24 kDa) (Figure 3b). Neither the apparent weight-average molecular weight data nor the Omega data from three different loading concentrations showed satisfactory overlap, indicating that the two species were not in chemical equilibrium. Analysis of the concentration distribution in terms of two nonequilibrating species indicated that the peak 2 samples comprised approximately 70% dimer and 30% monomer, in good agreement with the behavior of peak 2 in nondenaturing gel electrophoresis (cf. Figure 2, lanes 3, 7). These proportions, as estimated by both sedimentation equilibrium and gel electrophoresis of peak 2, were stable for days in 0.1 M NaCl at 5 °C, and chemical equilibrium was not reached at these temperatures. In 50% glycerol at –20 °C, the compositions of the isolated peak 1 and peak 2 material remained stable for at least 6 months.

In Tris buffers of very low ionic strength (5 mM Tris, pH 7.5) without supporting electrolyte, sedimentation equilibrium experiments were so confounded by nonideality that no sound interpretations could be made. But even without any NaCl, the heterogeneity of peak 2 material could be detected in 40 mM Tris at 5 °C (not shown).

Effect of Temperature on the Oligomeric State of D- α -14. Monomer and dimer did not interconvert appreciably at temperatures below 10 °C either with or without the addition of 0.1 M NaCl to the Tris buffer routinely used in our experiments. On raising the temperature above 20 °C, a slow monomer–dimer equilibrium reaction occurred.

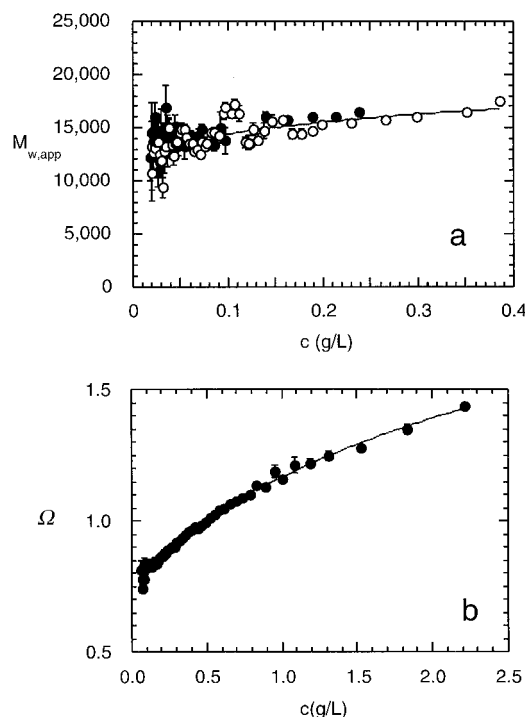


FIGURE 4: Sedimentation equilibrium at 30 °C of peak 1 and peak 2 material in 40 mM Tris-HCl, pH 7.5, in the presence of added 0.1 M NaCl. (a) With increasing concentration, both peak 1 (○) and peak 2 (●) material showed a gradually increasing molecular mass from approximately 12 kDa, indicating that the sample was associating weakly. The results were independent of whether peak 1 or peak 2 were used. The line is the best fit to a monomer–dimer model with $M_1 = 12\,500 \pm 500$, and $K_2 = (12.5 \pm 3.5) \times 10^3 \text{ M}^{-1}$. (b) Omega analysis of peak 1 material at 30 °C also shows clear evidence of association behavior by the upward curvature. The data from three different loading concentrations showed excellent overlap, and the pooled data gave a good fit to a nonideal monomer–dimer model, with an equilibrium constant of $12 \times 10^3 \text{ L/mol}$. Data points represent the mean values \pm SE of pooled data taken three points at a time.

Thus, incubation of peak 2 material at temperatures above 20 °C brought about a striking reduction in the apparent weight-average molecular mass. This effect occurred more rapidly at higher temperatures. After centrifugation for 24 h at 30 °C, peak 2 material underwent dissociation, and peak 1 material underwent association, such that the apparent weight-average molecular weight and Omega distributions were well-defined functions of the total concentration. The apparent weight-average molecular weight increased gradually through the cell, and these distributions were independent of whether peak 1 or peak 2 was the starting material (Figure 4a). Data from different initial loading concentrations all overlapped satisfactorily, indicating that chemical equilibrium was attained. Both the apparent weight-average molecular weight and Omega distributions were fitted well with a nonideal monomer–dimer model (Figure 4a,b). The weight-average molecular weight data of Figure 4a were fitted with a nonideal monomer–dimer model with M_1 of $12\,500 \pm 500$ (in good agreement with the actual molecular weight of 12 715 derived from the known sequence) and with a dimerization constant of $(12.5 \pm 3.5) \times 10^3 \text{ M}^{-1}$ (in good agreement with that obtained from fitting the Omega distribution). Chemical equilibrium was also achieved eventually at 20 °C (not shown), but the process was slower than at 30 °C and complete equilibrium required up to 36 h.

Nondenaturing gel electrophoresis confirmed the equilibrium observed by sedimentation equilibrium. At temperatures ≥ 20 °C, the peak 2 material showed substantial conversion of the slower moving dimer band to the faster moving monomer form (Figure 2, lanes 4, 8). Similarly, incubation of peak 1 material above 20 °C showed conversion of some of the faster moving monomer band to the slower moving dimer form (Figure 2, lanes 2, 6). Thus, after warm incubation, both peak 1 material and peak 2 material attained a similar equilibrium between the monomer and dimer bands (Figure 2, compare lanes 2 and 4 and lanes 6 and 8).

The concentration distributions at equilibrium were analyzed by means of the program NONLIN, and the distributions of $M_{w,app}$ and Omega were also analyzed as functions of concentration. By all three methods of analysis, the data were described most satisfactorily in terms of a nonideal monomer–dimer reaction. By all methods of analysis, and over a number of separate experiments, the equilibrium constant for the reaction in 40 mM Tris + 0.1 M NaCl at pH 7.5 and at 30 °C was between 1×10^4 and $3 \times 10^4 \text{ L/mol}$; data from a single experiment in which three separate concentrations were analyzed by the NONLIN method yielded a value of $1.2 \times 10^4 \text{ L/mol}$ (8.9×10^3 to $16.4 \times 10^3 \text{ L/mol}$, 95% confidence limits). The second virial coefficient, B , a measure of the nonideality, was between 1×10^{-6} and $2 \times 10^{-6} \text{ L mol g}^{-2}$. Temperature showed little effect on the equilibrium constant. Although the values at 30 and 37 °C tended to be greater than that at 20 °C, the difference was within the sample-to-sample variation.

Effects of pH and Ionic Strength. Over the range of pH 6.0–8.5, and over the range of ionic strength from 0.05 to 1.5 mol/L, the data appeared to be very similar, and were all fitted well by a nonideal monomer–dimer model. The equilibrium constant for the reaction appeared to be independent of pH between 6 and 8.5, and independent of ionic strength between 50 mmol/L and 1.5 mol/L (data not shown). While there may be a decrease in the equilibrium constant as the ionic strength is lowered below 50 mmol/L, the sharply increasing nonideality at these low ionic strengths, coupled with the imprecision inherent in the measurements, precluded accurate assessment.

Effect of Freeze-Drying. Sample that had been freeze-dried showed a slow reestablishment of equilibrium. Both peak 1 and peak 2 material initially showed poor overlap of $M_{w,app}$ versus concentration from different initial loading concentrations at 20 °C, indicating that both samples were heterogeneous and comprised substantial amounts of both monomer and dimer. Provided that dithiothreitol was present, equilibrium eventually appeared to be achieved at 30 °C, as judged from the satisfactory overlap of the Omega distributions, independent of the starting material. The parameters of this equilibrium reaction were indistinguishable from those of samples that had not been subject to freeze-drying.

Two-Segment Fragment, D- α -14,15. The behavior of the two-segment fragment of spectrin, D- α -14,15, was remarkably similar to that of the single unit. This protein also emerged from ion exchange chromatography on Mono-Q as two peaks. The first peak gave rise to a distinct, presumably monomer, band in nondenaturing gels, while the second peak gave rise to a major slower moving, presumably dimer,

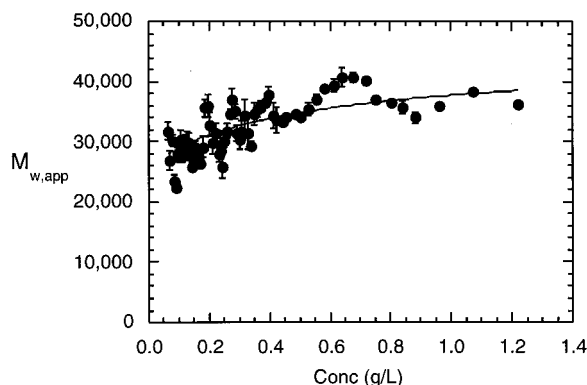


FIGURE 5: Apparent weight-average molecular weight distributions at combined sedimentation and chemical equilibrium of peak 1 for D- α -14,15 at 30 °C in 20 mM Tris-HCl at pH 7.5 with 0.1 M NaCl as supporting electrolyte. Data points represent the mean values \pm SE of pooled data, from three different loading concentrations, taken seven points at a time. The line is the best fit to the data, with $M_1 = 25\,000 \pm 1700$, and $K_2 = (26.8 \pm 3.3) \times 10^3 \text{ M}^{-1}$.

species, as well as a small amount of the faster moving band (not shown).

As with the single segment protein, sedimentation equilibrium experiments showed that chemical equilibrium between monomer and dimer was kinetically limited below 20 °C. Equilibrium was achieved at temperatures between 20 and 37 °C, with the $M_{w,app}$ and Omega distributions overlapping at a given temperature, independent of the starting material, its initial loading concentration, and the angular velocity. In the presence of 0.1 M NaCl at 20 °C, the data were fitted well with a nonideal monomer–dimer model with an equilibrium constant of approximately $3 \times 10^4 \text{ M}^{-1}$ at 20 °C, a monomer molecular weight of $25\,000 \pm 1700$, and a second virial coefficient $B = 3 \times 10^{-6} \text{ L mol g}^{-2}$ (Figure 5).

In the absence of supporting electrolyte, the nonideality of this fragment was relatively enormous and dominated the changes in the apparent weight-average molecular weight. Nevertheless, even under these conditions, the data were fitted well with a nonideal monomer–dimer reaction by all methods of analysis, yielding an equilibrium constant of approximately 10^4 M^{-1} between 20 and 37 °C.

Sedimentation Velocity Analyses. Sedimentation velocity analysis of both peak 1 and peak 2 of D- α -14 at 60 000 rpm revealed an apparent single boundary in each case. Nevertheless, analysis of the distribution of the apparent sedimentation coefficient, $g(s^*)$ (Stafford, 1992, 1994), revealed bimodality in the profiles, and extrapolation of these distributions from different times to $1/t = 0$ (Stafford, 1992) resolved two distinct sedimentation coefficients, particularly with peak 2 (Figure 6): a slower moving boundary with an $s_{20,w}$ of approximately 1.5 S, and a faster moving boundary with an $s_{20,w}$ of approximately 2 S. Peak 2 protein yielded predominantly the 2S species, with smaller amounts of the 1.5S species, while peak 1 protein yielded predominantly the 1.5S species.

Simultaneous fitting of up to nine scans at a time by means of the program SVEDBERG also resolved two separate species (Figure 7). Although the data were fitted reasonably well with a single sedimenting species, residuals showed sigmoidal trends. Fitting with two species provided a lower value of χ^2 , and sets of residuals that did not show sigmoidal trends. A sample of D- α -14 (0.54 g/L) that was found to

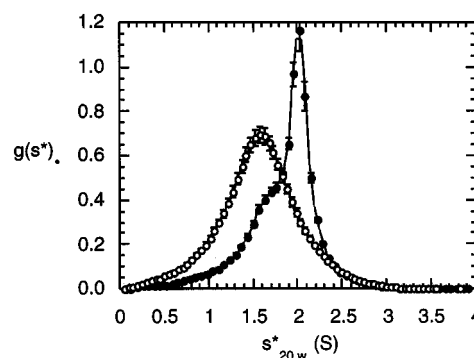


FIGURE 6: Distribution of the apparent sedimentation coefficient for peak 1 (○) and peak 2 (●) protein at 60 000 rpm. Sedimentation coefficients were corrected for the density and viscosity of the buffers, and are quoted as $s_{20,w}$ values. The $g(s^*)$ distributions were extrapolated to infinite time by the use of eq 7 of Stafford (1992).

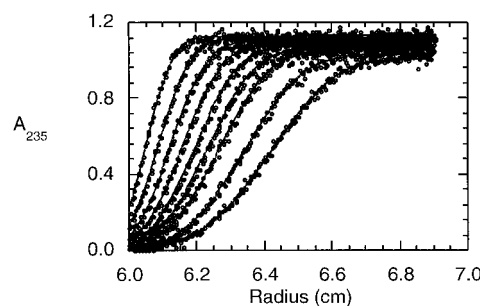


FIGURE 7: Sedimentation velocity analysis of peak 2 of D- α -14 (0.54 g/L) at 60 000 rpm and 20 °C. The points represent the measured absorbances at 235 nm, and the lines are the best fits to a model in which two species sediment independently.

Table 1: Hydrodynamic Properties of the *Drosophila* Spectrin Fragments and Their Oligomers

| species | $s_{20,w}$ (S) | M_r | f/f_0 |
|----------------------------|-----------------|------------------|-----------------|
| D- α -14 monomer | 1.58 ± 0.04 | 12000 ± 800 | 1.20 ± 0.03 |
| D- α -14 dimer | 1.97 ± 0.09 | 22900 ± 2000 | 1.53 ± 0.08 |
| D- α -14,15 monomer | 1.95 ± 0.10 | 25100 ± 1800 | 1.54 ± 0.08 |
| D- α -14,15 dimer | 2.63 ± 0.16 | 45000 ± 3200 | 1.87 ± 0.12 |

comprise approximately 90% monomer and 10% dimer by means of sedimentation equilibrium experiments was centrifuged at 60 000 rpm and 20 °C in the XL-A ultracentrifuge. The best-fit parameters indicated the presence of 87% monomer and 13% dimer, consistent with sedimentation equilibrium results. Similar studies of D- α -14 at 4 °C, at which temperature interconversion of the oligomers was negligible, were also consistent with the coexistence of monomer and dimer as separately sedimenting species.

The two-repeat unit, D- α -14,15, also revealed the presence of resolvable boundaries for separate monomer and dimer, in 20 mM Tris-HCl, pH 7.5, containing 0.1 M NaCl at 20 °C, and again the proportions of the species reflected the composition of the equilibrium mixture before the start of sedimentation.

The molecular weight values and frictional ratios of the various species were calculated from their sedimentation and diffusion coefficients (Table 1) and were in good agreement with the values expected on the basis of the sequence. The concentration dependence of the sedimentation coefficient for the D- α -14 monomer was not large, consistent with its proposed globular nature: at 0.7 g/L, $s_{20,w}$ was 1.58 ± 0.04 S while at 0.14 g/L, $s_{20,w}$ increased to 1.62 ± 0.04 S; i.e., the two dilutions were not significantly different. But the

concentration dependence of the sedimentation coefficient for the D- α -14,15 monomer was significant, consistent with D- α -14,15's more elongate structure: at 0.7 g/L, $s_{20,w}$ was 1.85 ± 0.04 S, while at 0.14 g/L, $s_{20,w}$ increased to 2.07 ± 0.01 S.

DISCUSSION

The present study has revealed the presence of reversible self-association reactions involving the D- α -14 and D- α -14,15 repeat units of spectrin. The presence of this association reaction in the 14th repeat unit provides an explanation for a dimer in the X-ray crystal structure of this protein. Presumably, the dimer crystallized more readily than the monomer in the study of Yan *et al.* (1993).

The equilibrium between monomer and dimer was independent of pH over the range pH 6–8.5, and independent of ionic strength over the range 0.05–1.5 M (within the precision of measurement). The reaction appeared to be enhanced weakly by increasing temperature, indicating that the reaction may be entropy-driven.

While the equilibrium constant was only weakly dependent on environmental variables, the kinetics of the process were markedly affected by temperature. The individual oligomers were kinetically trapped at low temperatures, and relaxation to equilibrium was enhanced only above 20 °C. The finding of a temperature-dependent conformation change has intriguing parallels with intact erythrocyte spectrin (Ralston *et al.*, 1977; Ungewickell & Gratzer, 1978). The large enthalpy of activation in both cases is likely to be due to the disruption of substantial helix–helix contacts that must precede association or dissociation.

The self-association reaction presumably involves unfolding the C helix from the A and B helices in the monomer, disrupting stabilizing interactions in the process, and then re-forming these interactions intermolecularly between the two monomers that form a dimer. Because interactions broken within the monomer are re-formed in the dimer, the association reaction will be largely isoenthalpic. The cost of this process, in terms of translational and rotational entropy, must be paid for by greater stability of the continuous BC helix compared to the arrangement where the C helix folds back on the B (and C) helix with the amino acids between the B and C helices forming a loop. It is interesting and puzzling that evolution has selected a sequence between the B and C helices that is in a less energetic state (i.e., has greater stability) when packed as part of a continuous BC helix than when forming a loop as in the native, intact protein.

The dimerization of D- α -14 was accompanied by a standard change in the Gibbs free energy, ΔG° , of -24.2 kJ mol $^{-1}$ at 30 °C. A van't Hoff plot was found to be approximately linear over the limited temperature range of 20–37 °C, yielding $\Delta H^\circ = +82.3$ kJ mol $^{-1}$ and $\Delta S^\circ = +351$ J mol $^{-1}$ K $^{-1}$ at 30 °C. It must be stressed that these thermodynamic parameters do not reflect the energy of interaction between the A, B, or C helices, but instead reflect small rearrangements in the folding of the molecule that accommodate dimerization. The positive sign of both the enthalpy and entropy changes may indicate enhanced hydrophobic interactions in the dimer compared with the monomer. Although we detected a curvature in the van't Hoff plot (not shown) that may indicate a decrease in heat

capacity (consistent with hydrophobic interactions), quantifying the curvature was compromised by the limited temperature range available and the limited precision of the data.

The magnitude of the equilibrium constant, 3×10^4 M $^{-1}$, while not particularly large, is such that at 1 g/L 60% of the protein would be present as dimer. The magnitude of the equilibrium constant for the association of the two-segment unit, D- α -14,15, was found to be similar to that of the one-segment unit, within the limits of experimental precision. This indicates that, in the absence of steric effects, and neglecting the entropic contributions due to the larger protein, the association interface may be similar in both polypeptides.

For both polypeptides, the sedimentation equilibrium results were adequately described by a nonideal monomer–dimer reaction; no significant improvement in fits was obtained by taking into account higher oligomers. For the one-segment unit, this suggests that both potential association sites (the exposed C-helix and the vacant site between the A and B helices) in both participating monomers are satisfied simultaneously.

The coexistence of the oligomeric species without significant interconversion at low temperatures allowed characterization of the hydrodynamic properties of the various species. The frictional ratios obtained from the sedimentation velocity studies indicate that the monomer is relatively globular, with a frictional ratio of approximately 1.2. The hydrodynamic properties of the various species were modeled with arrays of contiguous spheres (García de la Torre, 1992, 1994), with the total volume of the spheres set equal to the volume of the protein (based on the partial specific volume and the molecular weight), and with the linear dimensions of the array in close agreement with the dimensions determined from the X-ray crystal structure of the dimer of D- α -14.

The hydrodynamic behavior of the monomer of D- α -14 could be closely modeled by an array of 15 spheres, representing the A, B, and C helices packed together (Figure 8). The frictional ratio of 1.2, determined experimentally for the monomer, closely matched that of monomer II in Figure 8. On the other hand, a model in which the C and B helices were in line (monomer I) grossly overestimated the frictional ratio of the monomer, confirming that in solution the C helix of the monomer must be packed against the A and B helices. The D- α -14 monomer could also be modeled adequately by a simpler array of three spheres of radius 10.6 Å.

The experimentally determined frictional ratios of both the D- α -14 dimer and the D- α -14,15 monomer indicate that the shapes of both of these species are similar and somewhat elongated. The frictional ratio of both species was closely modeled by an array of 30 spheres of radius 6 Å in 3 close-packed rows of 10 (or by a simpler linear array of 6 spheres of radius 10.6 Å), consistent with the D- α -14 dimer crystal structure. The experimental value of 1.53 for the frictional ratio was reasonably close to that of 1.40 predicted by the model. On the other hand, a lateral association between monomers, as shown in Figure 8, did not adequately predict the frictional ratio of the D- α -14 dimer or D- α -14,15 monomer.

The frictional ratio of the D- α -14,15 monomer is also consistent with the organization of this protein as a linear structure of twice the length of a D- α -14 monomer. Furthermore, the frictional ratio of the dimer of D- α -14,15

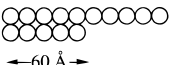
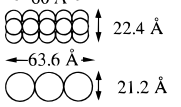


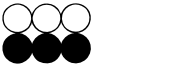
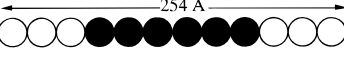
| Model | f/f_0 |
|--|---------|
|  Monomer I | 1.54 |
|  Monomer II | 1.19 |
|  I D-α-14 Dimer and | 1.41 |
|  II D-α-14,15 Monomer | 1.40 |
|  Lateral D-α-14 dimer | 1.17 |
|  D-α-14,15 Dimer | 1.76 |

FIGURE 8: Modeling the gross conformation of the spectrin fragments and their oligomers with arrays of contiguous spheres. The monomer of the single homologous unit, D-α-14, was modeled as an array of 15 spheres of 6.0 Å radius, either in 2 rows of 10 and 5 spheres, respectively, aligned at 1 end (monomer I), representing the subunit within the dimer, or as 3 close-packed rows of 5 spheres (monomer II), modeling the putative structure as predicted within the intact spectrin molecule. A cruder representation of monomer II, with essentially the same predicted properties, was achieved with a row of three spheres of 10.6 Å radius. The D-α-14 dimer and the D-α-14,15 monomer, with experimentally indistinguishable hydrodynamic properties, were modeled as two units of monomer II joined end-to-end. Again, a simpler representation comprising a linear row of six spheres of 10.6 Å radius provided an adequate description. An attempt to model the dimer as a lateral association grossly underestimated the frictional ratio. The D-α-14,15 dimer could be best represented as a linear array of 12 spheres of radius 10.6 Å.

indicates a substantially elongated molecule, consistent with four linear, end-to-end repeat units. A linear array of 12 spheres of radius 10.6 Å predicted the hydrodynamic properties of the D-α-14,15 dimer, within experimental uncertainty.

Since low temperatures kinetically stabilize the oligomeric structures, it is not easy to predict at what point during the preparation dimerization, clearly seen in peak 2, took place. While dimerization may be enhanced by the ion exchange chromatography step during isolation of the protein, it is more likely that association occurs as protein is synthesized during growth of the bacteria at 37 °C. The present results indicate that equilibration proceeds at a significant rate at 37 °C, and

there is no reason *a priori* to expect that fusion with GST would inhibit D-α-14 association. Indeed, GST is itself a dimer, and self-association of GST constructs via the fusion peptide has been reported (Riley *et al.*, 1995).

Our results suggest that structure analysis of spectrin's conformational segments by NMR methods will be difficult. While the D-α-14 monomer appears to be an ideal candidate for NMR analysis (relatively low molecular weight and substantial α-helix content), its tendency to self-associate, particularly at the high concentrations required for NMR studies, will make interpretation of the data difficult. Studies in low ionic strength and at low concentration may well mask a substantial tendency to association.

REFERENCES

- García de la Torre, J. (1992) in *Analytical Ultracentrifugation in Polymer Science and Biochemistry* (Harding, S. E., Rowe, A. J., & Horton, J., Eds.) pp 333–345, The Royal Society of Chemistry, Cambridge, U.K.
- García de la Torre, J., Navarro, S., Lopez Martinez, M. C., Diaz, F. G., & Lopez Cascales, J. J. (1994) *Biophys. J.* 67, 530–531.
- Johnson, M. L., Correia, J. A., Yphantis, D. A., & Halvorson, H. R. (1981) *Biophys. J.* 36, 575–588.
- Milthorpe, B. W., Jeffrey, P. D., & Nichol, L. W. (1975) *Biophys. Chem.* 3, 169–176.
- Morris, M. B., & Ralston, G. B. (1985) *Biophys. Chem.* 23, 49–61.
- Philo, J. (1994) in *Modern Analytical Ultracentrifugation* (Schuster, T., & Laue, T. M., Eds.) pp 156–170, Birkhauser, New York.
- Ralston, G. B., & Morris, M. B. (1992) in *Analytical Ultracentrifugation in Biochemistry and Polymer Science* (Harding, S. E., Rowe, A. J., & Horton, J. C., Eds.) pp 253–274, The Royal Society of Chemistry, Cambridge, U.K.
- Ralston, G. B., Dunbar, J. C., & White, M. D. (1977) *Biochim. Biophys. Acta* 491, 345–348.
- Riley, L. G., Ralston, G. B., & Weiss, A. S. (1996) *Protein Eng.* (in press).
- Schagger, H., & Jagow, G. V. (1987) *Anal. Biochem.* 166, 368–379.
- Speicher, D. W., & Marchesi, V. T. (1984) *Nature* 311, 177–180.
- Speicher, D. W., Morrow, J. S., Knowles, W. J., & Marchesi, V. T. (1980) *Proc. Natl. Acad. Sci. U.S.A.* 77, 5673–5677.
- Stafford, W. F., III (1992) in *Analytical Ultracentrifugation in Biochemistry and Polymer Science* (Harding, S. E., Rowe, A. J., & Horton, J. C., Eds.) pp 359–393, The Royal Society of Chemistry, Cambridge.
- Stafford, W. F., III (1994) *Methods Enzymol.* 240, 478–501.
- Teller, D. C. (1973) *Methods Enzymol.* 27, 346–441.
- Ungewickell, E., & Gratzer, W. B. (1978) *Eur. J. Biochem.* 88, 379–385.
- Winograd, E., Hume, D., & Branton, D. (1991) *Proc. Natl. Acad. Sci. U.S.A.* 88, 10788–10791.
- Yan, Y., Winograd, E., Viel, A., Cronin, T., Harrison, S. C., & Branton, D. (1993) *Science* 262, 2027–2030.

BI952224D